PAPER • **OPEN ACCESS**

Proof-of-concept of proton and photon measurements for large-area 2D dosimeters utilising optically stimulated luminescence

To cite this article: Jacob S. Nyemann *et al* 2023 *J. Phys.: Conf. Ser.* **2630** 012022

Journal of Physics: Conference Series **2630** (2023) 012022 doi:10.1088/1742-6596/2630/1/012022

Proof-of-concept of proton and photon measurements for large-area 2D dosimeters utilising optically stimulated luminescence

Jacob S. Nyemann[1], Mads L. Jensen[1], Lia B. Valdetaro[2,3], Morten B. Jensen[2,3,5], Rosana M. Turtos[1], Brian Julsgaard[1,4], Jørgen B. B. Petersen[5], Ludvig P. Muren[2,3,5] and Peter Balling[1,4]

[1]Department of Physics and Astronomy, Aarhus University, Denmark
[2]Department of Clinical Medicine, Aarhus University, Denmark
[3]Danish Centre for Particle Therapy, Aarhus University Hospital, Denmark
[4]Interdisciplinary Nanoscience Center (iNANO), Aarhus University, Denmark
[5]Department of Medical Physics, Aarhus University and Aarhus University Hospital, Denmark

E-mail: jacob1soegaard@phys.au.dk

Abstract. Reusable high-resolution 2D dosimeters have a great potential for radiotherapy verification and quality assurance, not least due to the reduced cost and simpler calibration procedures implied by reusability. We have performed proof-of-concept measurements in both photon and proton beams with a reusable 2D dosimeter (5×7 cm^2; 1 mm thickness) based on optically stimulated luminescence, using a readout setup scalable to 3D. Our data indicated a strong linear-energy-transfer quenching for this type of dosimeter.

1. Introduction

Development of dosimetry systems capable of measuring dose in 3D has been pursued in the past decades to improve radiotherapy dose verification and quality assurance procedures [1, 2, 3]. Such systems would increase the dimensionality of the measured data when assessing the quality of both machines and patient treatment plans. Our research group is contributing to this development by introducing a reusable system for 3D dosimetry that is based on optically stimulated luminescence (OSL) [4, 5, 6]. Transparent OSL-active 3D dosimeters can be stimulated by laser sheets in contrast to the head-on stimulation used for 2D dosimeters [7]. Creation of such dosimeters demands a precise match between the index of refraction of the OSL-active powder and the used matrix, particularly if the size of the OSL-active powder is not reduced to the nanometer scale [8, 9]. Further efforts include studying the properties of LiF:Mg,Cu,P (MCP) for its usage as the OSL-active component in such a dosimeter [10].

At present, radiotherapy dose measurements are mainly performed using point and 2D dosimeters, where high-resolution 2D dosimeters, e.g., radiochromic films, generally are one-time use. Thus, a reusable high-resolution 2D dosimetry system with limited need for re-calibration may be a great asset for the daily routines at radiotherapy clinics. Finally, an OSL-based 2D dosimeter could facilitate a future scaling to OSL-based 3D dosimeters.

In the following, we present proof-of-concept 2D readouts of a large 2D dosimeter, based on an OSL-active composite material in the form of OSL-active MCP powder embedded in a silicone matrix. The use of OSL allows for multiple repetitions of irradiation and readout of deposited dose, i.e., the 2D dosimeter is reusable. We present dose maps from both photon and proton irradiations acquired using a single 2D dosimeter multiple times. The optical system used for readout is further scalable to 3D.

2. Materials and methods

2.1. Samples

The 2D dosimeter used was prepared as a composite material with 30 wt% of MCP powder (grain size of 80 – 200 μm) acquired from RadPro embedded into a silicone matrix (SYLGARD™ 184 Silicone Elastomer with silicone/curing agent ratio of 10:1). The composite material was cured and cut into an approximately rectangular shape of 5×7 cm^2 with a thickness of ~1 mm. We note that the mixing method used here was unable to yield a homogeneous particle distribution for the dosimeter.

2.2. Irradiations

Photon irradiations were undertaken at Aarhus University Hospital (Aarhus, Denmark) with a Varian TrueBeam linear accelerator with 6 MV beam quality, 10×10 cm^2 jaw-defined field, dose rate of 6.0 Gy/min at the isocenter, and a source-to-axis distance of 100 cm. The photon beam was equipped with a flattening filter to provide homogeneous irradiation within $\pm$3 %. The dosimeter was placed between two 5 cm Solid Water® slabs and centered in the field with a source-to-surface distance of 95 cm, and a dose of 5.0 Gy at the isocenter was given.

The proton irradiation was delivered by a Varian ProBeam Proton Therapy System at the Danish Centre for Particle Therapy (Aarhus, Denmark). A dose rate of 20000 MU/min (65 Gy/min at beam entrance) was used to deliver a single spot of 77 MeV protons, yielding a dose of 4.3 Gy at the Bragg peak. The rectangular 2D sample was placed between two silicone blocks to approximate charged-particle equilibrium at the dosimeter position. A Monte Carlo simulation representative of this set-up was performed with TOPAS (version 3.2) [11], with a validated beam model.

All doses and dose rates are presented as water-equivalent doses. Fairly high doses were chosen to ensure sufficient signal over the entire dosimeter range for these proof-of-concept measurements.

2.3. Readout and calibration

A 445 nm laser with a maximum output of ~4.5 W was used for optical stimulation of the sample during readout. The laser beam was manipulated to create a truncated Gaussian field with stimulation intensity ranging from 5 mW/cm^2 to 46 mW/cm^2 in the sample region (lowest near corners). With sufficient readout time, the decaying OSL signal will reach background level, even in low-intensity regions, and the time-integrated signal will be largely unaffected by the intensity profile of the stimulation.

Measurements were acquired by imaging the emitted OSL onto the CCD sensor of the camera (SOPHIA 2048B, Princeton Instruments). Imaging was achieved with a Jenoptik APO Macro lens system, with a field-of-view resulting in an imaged area of $(9.67 \pm 0.05)^2$ cm^2, with each of the 256×256 (8×8 hardware-binned) pixels representing an object size of $(\sim 0.38\ \text{mm})^2$. Elimination of unwanted light (e.g., stimulation light) was achieved with a combination of four Ø 2" filters placed in front of the imaging system. Each measurement consisted of 26 consecutive frames using an exposure time of 60 s. The time between irradiation and readout ranged from 1 hour to 3.25 hours. All measurements are presented after background subtraction. Background measurements were performed after bleaching for ~30 minutes under 385 nm LEDs (3 – 40 mW/cm^2) followed by 5 minutes under the stimulating laser (the reasoning behind this bleaching procedure is described elsewhere [12]).

To demonstrate the potential of this type of dosimeter, we performed a calibration measurement to correct for the inhomogeneous particle distribution. The calibration matrix was constructed by dividing the planned photon dose (5 Gy) with the observed total signal (time-integrated) for each pixel of the dosimeter area. The main objective of the calibration was to correct for inhomogeneities in the

particle distribution, but by construction, it also converts from measured counts to dose levels. Thus, by using this calibration, the dose response is inherently assumed to be perfectly linear, unaffected by fading time, independent of dose rate, irradiation type (photon vs. proton), and linear energy transfer (LET). A clinically relevant calibration protocol must be more comprehensive to eliminate these assumptions.

3. Results and discussion

Figure 1 presents the detected OSL emitted from the 2D dosimeter after a homogeneous photon irradiation. The OSL signal curve of spatially integrated signal as a function of stimulation time, seen in Figure 1(a), shows a characteristic decaying behavior generally seen for OSL-based dosimeters as the OSL traps are emptied. The total OSL signal of the measurement is shown in Figure 1(b), found as the sum of all the frames taken during the measurement, yielding a signal map expected to be proportional to the given dose. However, with the dosimeter's inhomogeneous particle distribution, the signal response was inhomogeneous as well. Additionally, the (apparently) too short readout time used here caused an under response for corner regions (lowest stimulation intensity) unrelated to the particle distribution, an effect seemingly visible in especially the lower corners of Figure 1(b).

Figure 1(c) presents the same measurement after correction with the calibration matrix. After calibration, the dose map shows an almost uniform signal with a mean pixel value of (5.8 ± 0.4) Gy. Since the dose map in Figure 1(c) shows an elevated dose level (compared to the planned dose) and non-random variations, some (unidentified) systematic errors were not captured by our calibration with the current readout setup/procedure. This was most likely due to the many assumptions introduced with the simple calibration procedure used here.

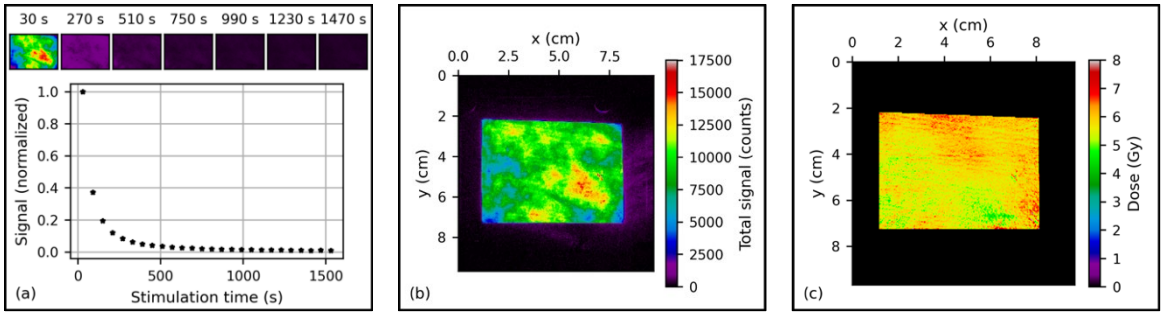

Figure 1. Spatially resolved 2D OSL readout of the rectangular 2D dosimeter uniformly irradiated by the photon irradiation. In (a), individual frames are shown on top, while the main graph shows a normalized OSL decay curve, where individual points are based on the sum of all pixels within the dosimeter area of a frame, e.g., the representative frames above. Time stamps are given as the centre of each captured frame. Panel (b) shows the measured 2D data given as a sum of all frames. Panel (c) presents the 2D measurement after applying the calibration matrix to the measured data.

In Figure 2, the calibrated 2D OSL distribution of the dosimeter following exposure to a single beam of protons is shown. The dose map shows the expected overall shape of a proton beam entering from the right with its fixed width, increased intensity in the central part of the beam, and increasing signal near the end of the track (the Bragg peak). With the line profiles shown in Figure 2(b), we see that these general trends are similar to that of a Monte Carlo simulation. However, the line profiles also highlight a clear under response near the Bragg peak. This is likely explained by quenching due to a high LET near the Bragg peak, which is a common issue encountered for proton dosimetry. This is consistent with the relatively strong quenching observed for the TL signal of MCP dosimeters [13]. Despite challenges with MCP particle distribution (possibly contributing to the distorted Bragg peak) and LET quenching, Figure 2 clearly shows the potential for a composite dosimeter material with readout based on OSL. In

particular, the present measurements highlight the scalability of 2D OSL dosimeters with our 5×7 cm^2 dosimeter and 9.67×9.67 cm^2 readout area, significantly larger than previously demonstrated [14, 15].

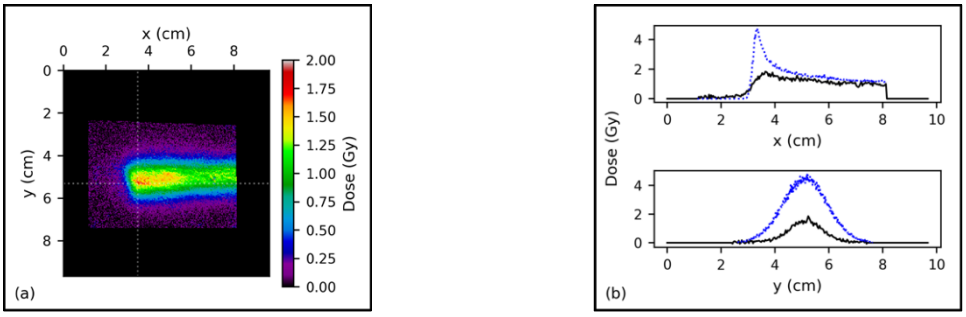

Figure 2: Panel (a) shows a 2D dose map of the rectangular 2D dosimeter irradiated by the described proton beam after adjustment with the calibration matrix. Horizontal and vertical line profiles of the 2D dose map (black lines) are shown in (b) alongside representative line profiles from a Monte Carlo based simulation, which are shown for comparison in blue.

4. Conclusion

We have shown proof-of-concept 2D measurements of photon and proton irradiation profiles using a composite MCP-silicone dosimeter. The proof-of-concept measurements were performed on a 5×7 cm^2 dosimeter, and read out with a setup capable of 9.67×9.67 cm^2 dosimeters. Finally, we showed that the OSL signal from micrometer-sized MCP powder exhibits significant quenching in high-LET regions of a proton beam, i.e., near the Bragg peak. Future research in this direction will include the study of LET quenching, improved calibration procedures, and consistency of readout.

5. Acknowledgements

This work was funded by the Independent Research Fund Denmark, Technology and Production Sciences and the Novo Nordisk Foundation and the. P S Skyt is acknowledged for his assistance regarding dose delivery from the proton beam facility at the Danish Centre for Particle Therapy.

6. References

[1] Doran SJ 2009 *Appl. Radiat. Isotopes* **67** 393-398
[2] Schreiner L J 2015 *J. Phys.: Conf. Ser.* **573** 012003
[3] Mijnheer B (ed) 2018 Clinical 3D dosimetry in modern radiation therapy
[4] Balling P *et al* 2018 European Patent Application EP3264137A1
[5] Nyemann J S *et al* 2022 *J. Phys.: Conf. Ser.* **2167** 012026
[6] Jensen M L *et al* 2022 *Sci. Rep.* **12** 8301
[7] Jensen M L *et al* 2022 *J. Phys.: Conf. Ser.* (This volume)
[8] Nielsen C L *et al* 2022 *J. Phys.: Conf. Ser.* (This volume)
[9] Nielsen C L *et al* 2022 *Nano Lett.* **22** 1566-1572
[10] Nyemann J S *et al* 2020 *Radiat. Meas.* **138** 106390
[11] Perl J *et al* 2012 *Med. Phys.* **39** 6818-6837
[12] Nyemann J S *et al* 2022. (In prep.)
[13] Olko P *et al* 2020 *Radiat. Prot. Dosim.* **192** 165-177
[14] Sadel M *et al* 2020 *Radiat. Meas.* **133** 106255
[15] Sadel M *et al* 2020 *Radiat. Meas.* **133** 106293